Application of **MODELLING** for **ENHANCED ULTRASONIC INSPECTION** of stainless steel welds

B. Chassignole, O. Dupond, T. Fouquet, A. Le Brun, J. Moysan and P. Benoist

ABSTRACT

The ultrasonic inspection of the primary coolant piping of Pressurized Water Reactors (PWR) is a major concern for the nuclear industry. Numerous studies have been undertaken over some years by EDF R&D in collaboration with the French Atomic Energy Commission (CEA) to improve the non-destructive testing (NDT) process for these applications and to help towards their qualification. More particularly, a great deal of work was carried out on the inspection of austenitic stainless steel welds. Indeed, the anisotropic, heterogeneous and coarse granular structures of these welds lead to important disturbances of the ultrasonic propagation: beam skewing and splitting, attenuation, backscattering and ghost echoes. This paper presents the methodology developed for modelling the ultrasonic inspection of austenitic welds, which is based on an accurate characterization of the material. Two numerical approaches are presented: a finite elements code, ATHENA, developed by EDF, and a semi-analytical code that is a part of the CIVA simulation platform developed by the CEA. These codes simulate the propagation of the ultrasonic beam in the weld and calculate the defect-beam interaction. Ultrasonic beam disturbances are illustrated from experimental and numerical results for different applications. In particular, the influence of variations in the weld structure on NDT performance is discussed. This comparison between experiment and modelling shows the modelling methodology to be valid.

IIW-Thesaurus keywords: MMA welding; Austenitic stainless steels; Ultrasonic testing; Simulating.

1 Introduction

Numerous multipass welds in austenitic stainless steel are present on the primary and auxiliary systems of nuclear power plants with pressurized water reactors. These welds are characterized by columnar grains which grow in relation to the direction of the thermal gradient and whose orientation changes according to the position in the weld. The solidification structure is then anisotropic and heterogeneous.

It was demonstrated that this particular columnar structure leads to disturbances of the ultrasonic propagation, such as deviation and division of the ultrasonic beam [1-3]. On the other hand, the grain size is sometimes similar to the wavelength which may introduce high levels of attenuation and structural noise.

EDF (Electricité de France), in collaboration with the CEA (French Commission of Atomic Energy), undertook numerous studies in order to evaluate the ultrasonic controllability of those welds, to improve the NDT process for these applications and to help towards their qualification [4-6]. Modelling tools are especially useful to improve the understanding of the phenomena.

This paper is devoted to the methodology developed to simulate the ultrasonic inspection of austenitic welds, which is based on an accurate characterization of the material. The weld descriptions and material input parameters for modelling will be discussed in detail.

Two numerical approaches are presented: a finite elements code and modelling tools relying on semi-analytical solutions. Experimental and modelling results are compared for a specific configuration. Results are then discussed both qualitatively (description of the echoes on B-scan presentations) and quantitatively (echo amplitudes, defect sizing).

2 Weld characteristics and characterization

This study was performed on mock-ups representative of AISI 316L industrial austenitic stainless steel welds. They were made using a manual shielded metal arc welding (SMAW) process with ESAB OK 63-25 electrodes. The measured chemical composition is given in Table 1.

The weld structure is characterized by a dendritic type growth parallel to the heat flow direction, whereas the wrought base metal exhibits an equiaxed structure with small grain size. The weld metal contains about 8 % of

Doc. IIW-2150, recommended for publication by Commission V "Quality Control and Quality Assurance of Welded Products."

Table 1 – Measured chemical composition of OK 63-25 electrode [wt. %]

C	Mn	P	S	Si	Ni	Cr	Mo	Co	Cu
0.02	1.3	0.01	0.01	0.3	12.4	19.4	2.4	0.03	0.02

primary ferrite in a skeletal structure lying at the dendrite core. The size of this skeletal ferrite is far smaller than the ultrasonic wave length and so the ultrasonic propagation is mainly affected by the austenitic phase. In the event of sufficiently low welding energy, this solidification mode leads to elongated and oriented grains, which can grow by an epitaxial and selective growth process over several millimetres length. An example of such a structure is shown in Figure 1 for a weld with a K-chamfer and backwelding, corresponding to a set-in branch pipe on the primary system of a nuclear power plant. The piping thickness is equal to 69 mm.

The three macrographs corresponding to mock-ups welded by three different welders reveal some variations of the weld structure. Structural variations along the welding direction, leading to variations in ultrasonic propagation, were also highlighted in austenitic stainless steel welds [7].

The crystallographic texture of the material was characterized by various techniques, including X-Ray diffraction or Electron BackScattering Diffraction (EBSD) [8]. EBSD analyses are illustrated in Figure 2 for a square sample of 4 x 4 mm^2 covering two welding runs. W, T and V axes

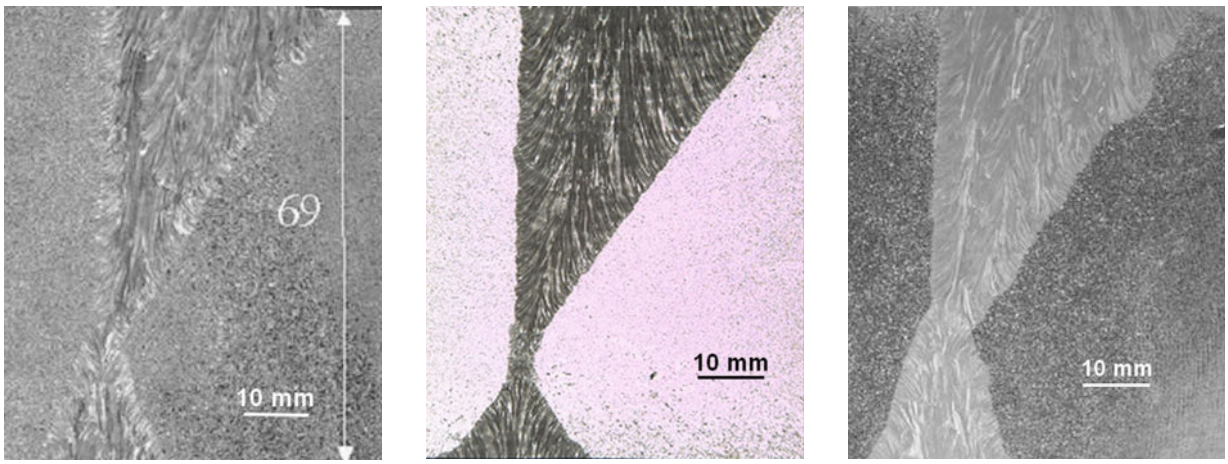

a) Mock-up A b) Mock-up B c) Mock-up C

Figure 1 – Grain orientation measurement in a set-in branch pipe weld

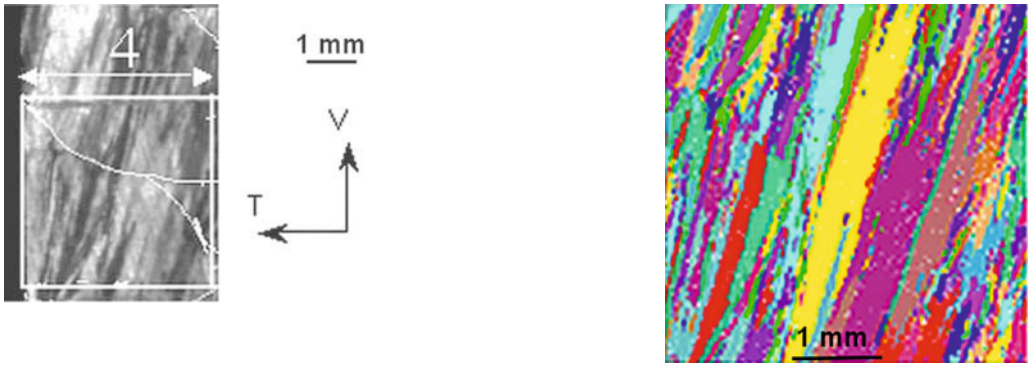

a) Sample analysed b) Grain colour map

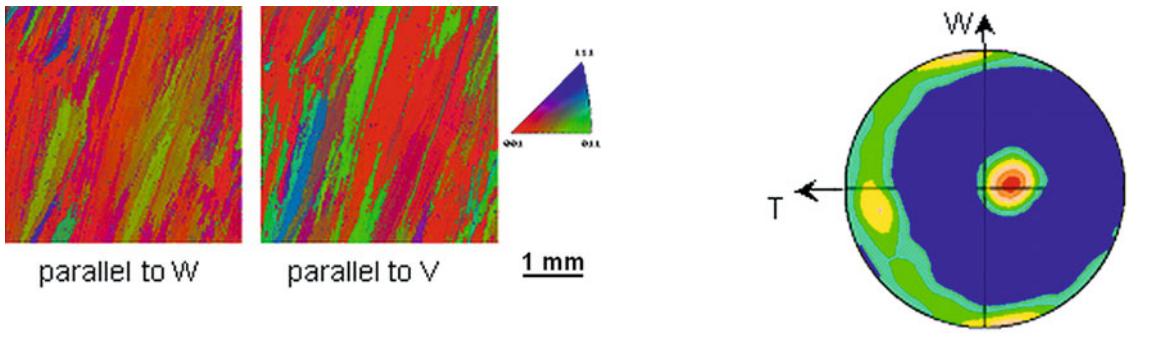

c) Inverse pole figure map for crystal direction parallel to W and to V d) Calculated pole figure for {200} plane

Figure 2 – EBSD analysis on an austenitic stainless steel weld

correspond respectively to welding, transverse and vertical directions. The {200} calculated pole figure highlights a crystallographic texture characteristic of an orthotropic symmetry and with a fibre axis slightly misaligned with the V axis. Grain size can also be estimated: grain width average is about 200 µm and grain length can reach several millimetres.

The orientation of the long axis of the columnar grains, which is directly linked to the crystallographic fibre axis, can be estimated from image processing performed on the images shown on Figure 1. This approach is valid only if the grain disorientation along the welding direction is null (i.e. the (TV) plane is a material symmetry plane), which is the case for this weld, realized in a flat position.

When the weld structure is not accessible for metallographic examination, the local direction of grains in a weld can also be calculated with the MINA model. MINA was developed to describe the structural heterogeneity of a multipass shielded metal arc weld [9]. This model is based on parameters connected to the welding process (weld run inclinations and remelting rates) and on the information extracted from the welding notebook geometry of the chamfer, number of weld runs and series order, diameters of electrodes used for each weld run etc.). A comparison between image processing and MINA results for the set-in branch pipe weld is illustrated in Figure 3. The cell size is equal to 2 x 2 mm^2. Note that the structure heterogeneity and dissymmetry are well described by MINA. In particular, this model will be useful to perform parametric studies on the influence of weld structure variations.

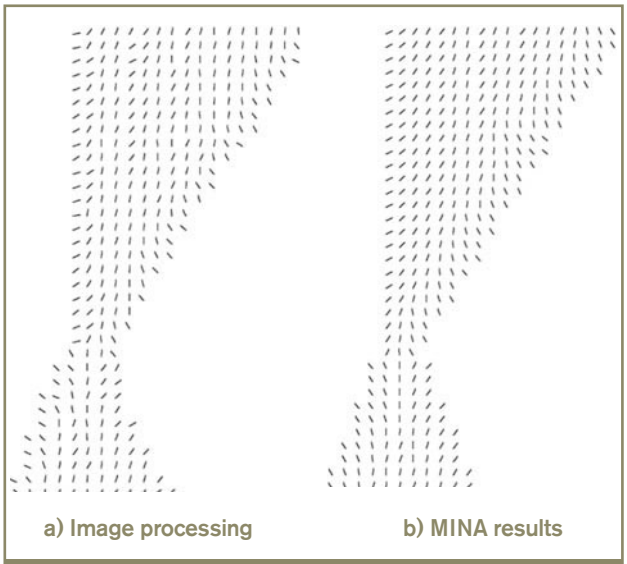

Figure 3 – Grain orientation measurement in a set-in branch pipe weld

3 Modelling codes

3.1 Generalities

The modelling study is based on two complementary approaches, permitting simulation of the propagation of the ultrasonic waves in anisotropic and heterogeneous complex media and the interactions of the beam with defects of complex geometry.

The ATHENA 2D code, developed by EDF R&D, solves the elastodynamic equations, expressed with the stresses and the velocities of the displacements by a finite elements method [10]-[11]. The numerical methods of a finite element or finite differences approach the exact equations that represent the physical phenomena and give, in particular, quantitative information on the energy of the signals. The error does not depend on the number of media crossed by the wave, thus multiple reflections are always taken into account. The development of a 3D version of this code is in progress.

Modelling tools incorporated in the CIVA simulation platform developed by CEA are used to model 3D configurations with reasonable computation time [12]-[13]. The models are based on semi analytical kernels and numerical integration, which allow the computation of beam propagation and flaw scattering in various cases. This makes it possible to predict the performance of an inspection in realistic industrial configurations for complex specimen geometries and with standard or phased arrays transducers. As far as ultrasonic propagation in an austenitic weld is concerned, the validation of semi-analytical models is still in progress.

In order to simulate the ultrasonic propagation in the weld, input data are required; in particular, realistic descriptions of the weld. It has been demonstrated that the welds can be described by a finite number of anisotropic but homogeneous zones which are characterized by the direction of the fibre axis and a set of elastic constants [4]-[5]. This type of description is illustrated in Figure 4.

An illustration of beam propagation modelling in an austenitic weld is shown in Figure 5. In this test configuration, a longitudinal probe with normal incidence and a frequency

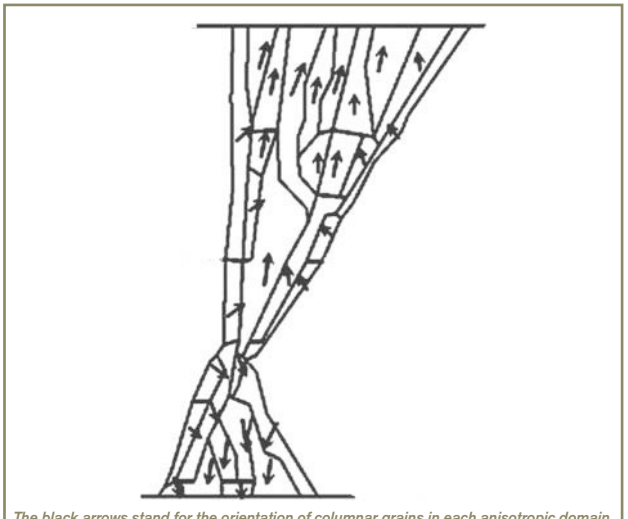

The black arrows stand for the orientation of columnar grains in each anisotropic domain.

Figure 4 – Example of description of an austenitic weld used in ultrasonic modelling codes

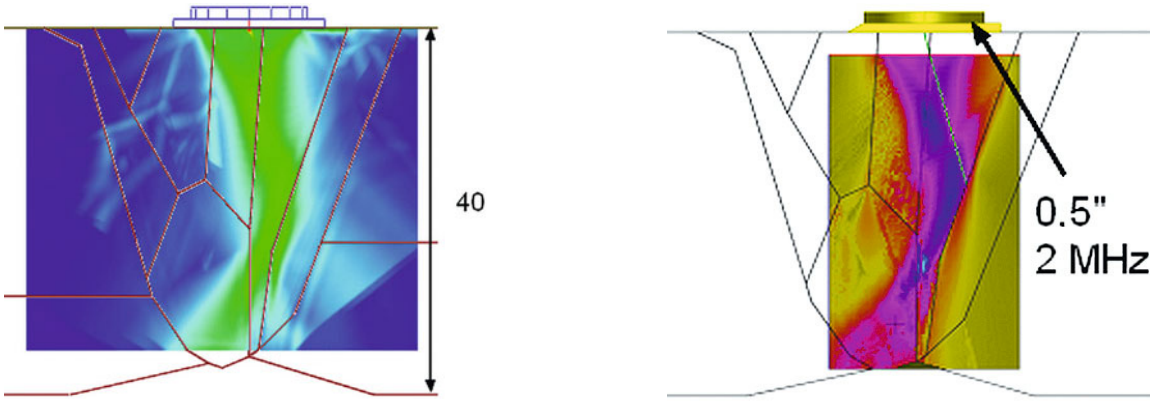

a) Finite elements modelling

b) Semi-analytical modelling

Figure 5 – Illustration of beam skewing in an austenitic weld (2 MHz probe)

of 2 MHz is located in the middle of a butt weld with a V-chamfer and 40 mm thickness. The weld structure is described by seven zones because it is less heterogeneous regarding the grain orientation than the structure of the K-chamfer weld in Figure 4. The double skewing of the beam due to the material anisotropy and the structural heterogeneity is clearly highlighted by both codes.

3.2 Modelling of ultrasonic scattering

As the wavelength of the ultrasonic waves is of the same order of magnitude as of the grain size, the waves can be strongly scattered at each grain boundary. This scattering leads to two specific phenomena: attenuation of the wave and structural noise. The latter is due to the backscattered waves intercepted by the probe and can lead to spurious echoes on the ultrasonic images. Because of these disturbances, the signal to noise ratio of defect echoes can be significantly reduced in comparison with inspection of the base metal (grain size close to 120 µm).

The attenuation due to grain scattering has been implemented in both codes. In the case of the finite elements code, the equations are as follows:

$$\frac{\partial \sigma}{\partial t} + D\sigma = C\varepsilon(v) \quad (1)$$

$$\rho \frac{\partial v}{\partial t} - div\sigma = f \quad (2)$$

where

σ is the stress tensor,

ε is the strain velocity tensor,

ρ is the density and

f is a strength source.

Tensor C is characteristic of the elastic constants whereas tensor D is characteristic of the attenuation coefficients. Tensors C and D are determined by an optimization process based on the adjustment of experimental data of ultrasonic velocities and attenuations for quasi-longitudinal and quasi-transversal waves [11]. Several studies have demonstrated that the variations in velocity and attenuation versus the angle between the beam direction and the grain orientation are characterized by anisotropic constitutive equations [14]-[16].

In the semi-analytical tools, an attenuation coefficient is associated with each ray during the calculation of the ultrasonic beam. The value of the coefficient depends on the direction of the ray relative to the grain orientation.

Work is also in progress to simulate the structural noise in the finite elements code. The approach consists in a grain scale modelling of the structure in each anisotropic and homogeneous domain defined in Figure 4 [17]. The average length and width of the austenitic grains must be estimated, for example, from EBSD analysis. Future work will carry out validation of this model.

4 Application for the ultrasonic examination of the set-in branch pipe weld

The different testing configurations are presented in Figure 6. Notches with heights from 5 to 30 mm were machined in the base metal and in the weld of the mock-up of Figure 1 a), which is representative of a set-in branch pipe weld. This mock-up was inspected with standard probes (single element and TRL probes) which produce 60° longitudinal waves at a frequency of 2 MHz [6], [18].

The experimental results are illustrated in Figure 7 with a comparison between B-scan images for notches in the isotropic base metal and in the weld. For the isotropic configuration, the notch detection is characterized by three echoes (diffraction, corner and LLT echoes) explained on Figure 8. The LLT echo corresponds to the following travel path: reflection of the longitudinal waves from the defect (LL mode) followed by a second reflection from the back

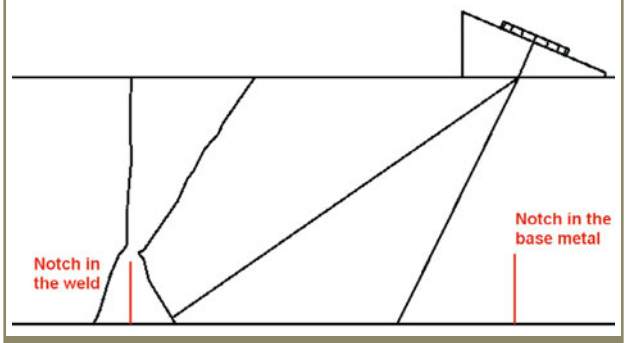

Figure 6 – Configurations of inspection of notches machined in a set-in branch pipe mock-up

wall producing a mode conversion to transversal waves (LT mode).

For the weld inspection, these images show that the anisotropic and heterogeneous structure leads to the presence of additional echoes (named "spurious echoes"). Moreover, beam deviations due to the weld structure lead to bad positioning of the defect indications. The errors in defect sizing, based on depth location of diffraction and corner echoes, are then greater than in the base metal.

Notch responses were predicted with both modelling codes. Modelling results are illustrated in Figure 9 and amplitudes of the diffraction and corner echoes for a notch of 15 mm height are given in Table 2. The reference defect is a notch of 10 mm height, machined in the isotropic base metal. A negative value in Table 2 denotes attenuation of the ultrasonic signal in the weld. Furthermore, the maximum experimental amplitude is indicated but a value

Table 2 – Amplitudes of corner and diffraction echoes for a 15 mm notch in the weld compared to the same echoes without weld (dB)

	Corner echo	Diffraction echo
Experiment	-6.5	-1
Finite elements modelling	-9.0	+1.5
Semi-analytical modelling	-9.0	+1

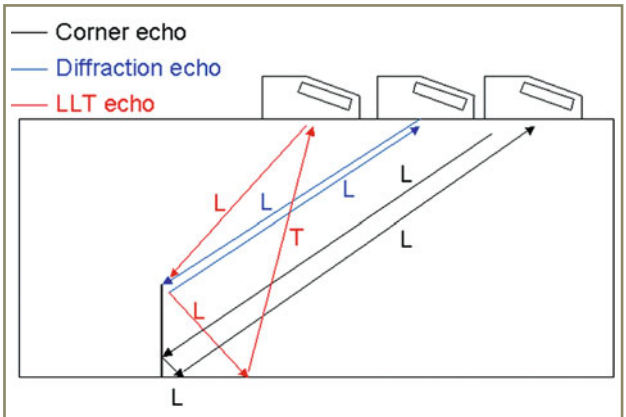

Figure 8 – Ultrasonic paths associated with corner, diffraction and LLT echoes

of –9 dB was found for the corner echo in the B-scan corresponding to the notch centre.

Both codes reproduce correctly the experimental amplitudes. The amplitude of the corner echo is low for notches in the weld because of the beam distortion and

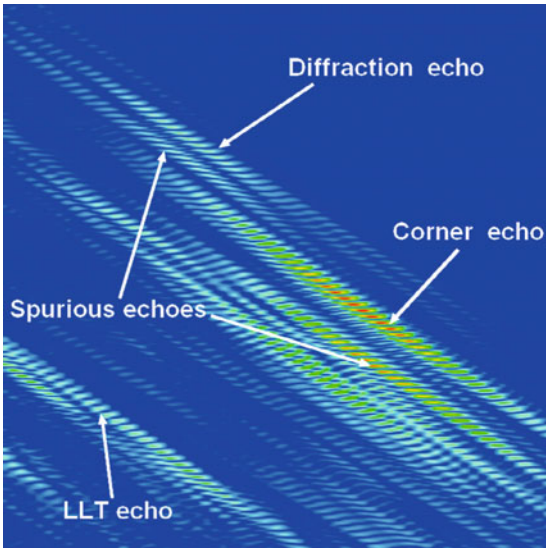

Figure 9 – B-scan presentations for a 15 mm notch in the weld (finite element modelling)

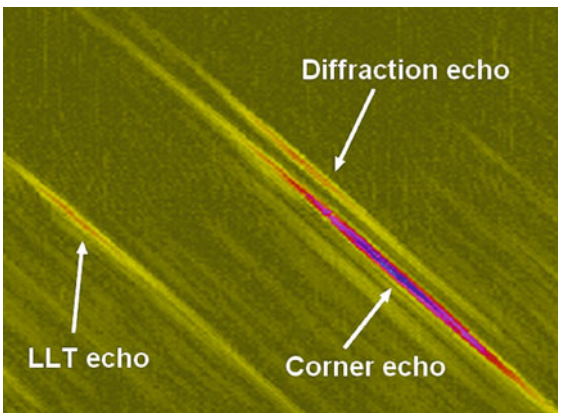

a) on the notch in the base metal

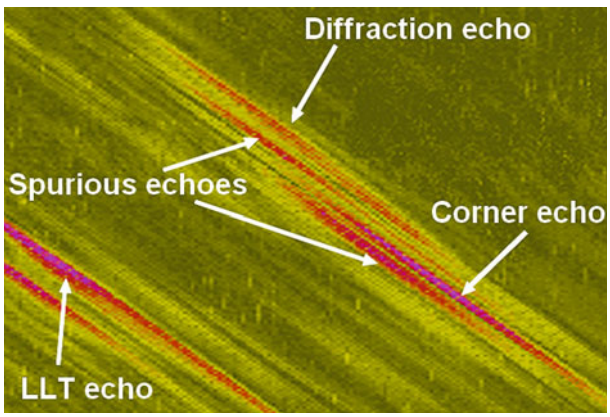

b) on the notch in the weld

Figure 7 – Experimental B-scan presentations – different echoes observed

attenuation. The amplitude of the diffraction echo is far more stable because the ultrasonic path in the weld is significantly shorter than for the corner echo (see Figure 6). However, a previous study showed that the amplitude of this echo for a 30 mm notch is 8 dB weaker than for a 15 mm notch because the ultrasonic path in the weld is greater to detect the 30 mm defect tip [18].

This study thus demonstrates that it is necessary to take into account the ultrasonic attenuation due to grain scattering in order to obtain realistic echo amplitudes. Analyses on other configurations with various austenitic stainless steel welds lead to a similar conclusion [11].

Moreover the finite elements code predicts the presence of spurious echoes. Thanks to modelling, these echoes were identified as complex trajectories in the weld with mode conversions of longitudinal and transversal waves in the presence of the defect [18]. Mode conversions through the chamfer and the interfaces of the weld structure are not simulated in the current semi-analytical tools. New developments will be incorporated in future versions of the semi-analytical tools to simulate these phenomena.

A parametric simulation study was also conducted with the finite element code to analyse the influence of variations in the weld structure on ultrasonic testing results. This was limited to the case of the notch of 15 mm height. Three weld descriptions were obtained from the images of Figure 1. Ten more descriptions were given by MINA, by varying the different input parameters of the model.

We therefore conclude that the variation in amplitude of the corner echo is about 4 dB, depending on the structure. Experimentally, the same value was found for defects machined at different locations along the welding direction of the mock-up. Moreover, the minimum amplitude of the corner echo in modelling is obtained for the weld description corresponding to the experimental configuration. It can therefore be concluded that the risk of obtaining a signal to noise ratio below the experimental value (5 dB) is low.

Furthermore, this specific study demonstrates that the conditions for occurrence of the spurious echoes depend on the characteristics of the structure (grain orientation, chamfer orientation, degree of heterogeneity). This conclusion is illustrated in Figure 10, with the comparison of B-scan presentations obtained for two different weld descriptions.

Finally, the sizing of notch heights based on the positioning of the diffraction and corner echoes was analysed. Errors between 1 and 3 mm are found, both in over-sizing and in under-sizing. These values are in agreement with those obtained experimentally. For a particular case, the simulation yields a sizing error of 5 mm. Moreover, for certain configurations, modelling predicts a spurious echo amplitude higher than the corner echo amplitude which may disturb the analysis.

5 Conclusions and outlook

This paper presents a methodology developed for modelling ultrasonic inspection of austenitic welds realized by the SMAW process. This methodology is based on an accurate characterization of the material. Different techniques of material characterization were used to provide input data (grain orientation, stiffness tensor, coefficients of attenuation) to modelling codes.

Experimental analysis on a mock-up with notches reveals disturbances of the ultrasonic inspection related to the anisotropic and heterogeneous structure of the weld: attenuation of echo amplitude due to grain scattering and beam distortion, errors in defect sizing due to the beam

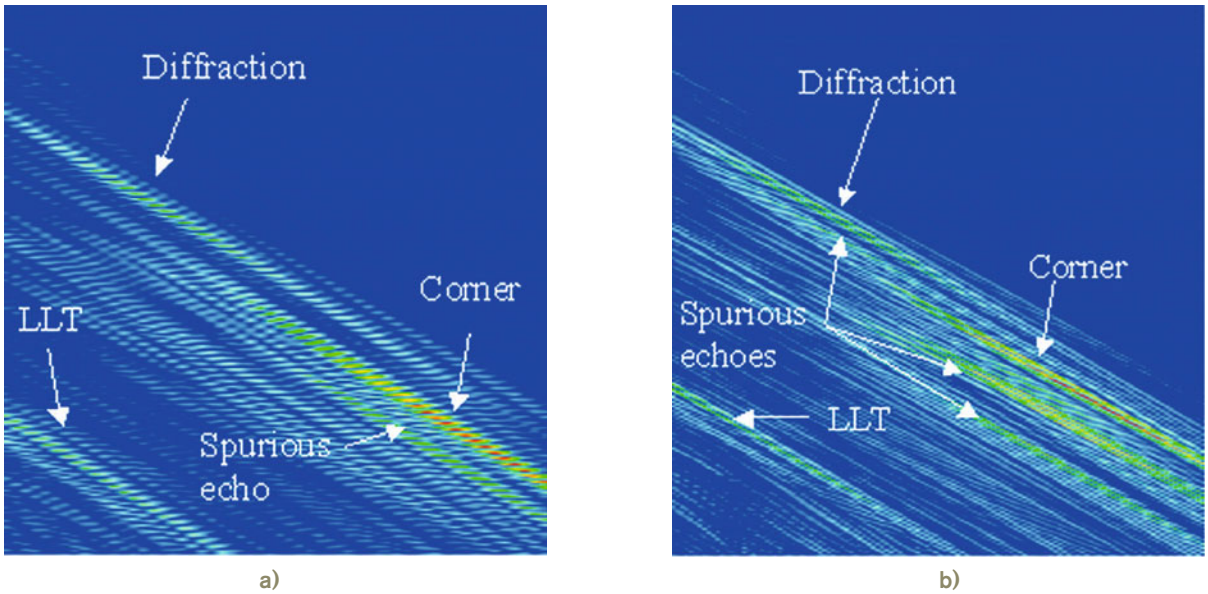

Figure 10 – B-scan presentations with the finite elements modelling for two different weld descriptions

skewing, presence of spurious echoes due to mode conversions in the weld.

Modelling, with two complementary approaches, allows prediction of these disturbances. The test configurations studied validate the methodology developed for SMAW austenitic welds. Taking into account the attenuation related to grain scattering makes it possible to obtain more pertinent simulation results regarding the amplitudes of the different echoes. The origins of spurious echoes were explained with finite elements modelling.

Validations of the models must be continued. In particular, future use of the 3D version of the finite elements code will permit the study of complex configurations (for example a plane defect tilted from the welding direction) and comparison with semi-analytical codes will be proposed for these cases. Mode conversions due to the weld structure, which are behind the spurious echoes, will be implemented in the semi-analytical tools.

Further work might be carried out to try to improve the performance of defect sizing. Work in signal processing is in progress to try to distinguish between echoes of interest and spurious echoes. On the other hand, methods of defect reconstruction are being developed in the CIVA software, taking into account the actual direction of the beam into the weld. This requires detailed knowledge of the structure of the weld but access to this information is not easy. An alternative consists in using the MINA model in order to simulate the local direction of grains. The study of the influence of variations in the weld structure on the propagation of ultrasonic waves of which details are given in this paper demonstrates the usefulness of this model in performing parametric studies.

Two further lines of work may be outlined:

1. To apply this approach with other SMAW electrodes. A comparison between experiment and modelling results for a welding mold in Inconel 182® has already been proposed [19].
2. To adapt this methodology to Gas Tungsten Arc Welding (GTAW) process.

References

[1] Tomlinson J.R., Wagg J.R. and Whittle J.M.: Ultrasonic inspection of austenitic welds, British Journal of NDT, 1980, vol. 22, no. 3, pp. 119-127.

[2] Langenberg K.J., Hannemann R., Kaczorowski T., Marklein R., Koehler B., Schurig C. and Walte F.: Application of modeling techniques for ultrasonic austenitic weld inspection, NDT&E International, 2000, vol. 33, no. 7, pp. 465-480.

[3] Halkjaer S., Sorensen M.P. and Kristensen W.D.: The propagation of ultrasound in a austenitic weld, Ultrasonics, 2000, vol. 38, no. 1-8, pp. 256-261.

[4] Chassignole B., Villard D., Nguyen Van Chi G., Gengembre N. and Lhemery A.: Ultrasonic propagation in austenitic stainless steel welds – approximate model and numerical methods results and comparison with experiments, Proceedings of Rewiew of Progress in QNDE, July 1999, vol. 20A, Montreal, pp. 153-160.

[5] Dupond O., Chassignole B., Doudet L. and Birac C.: Methodology for modelling ultrasonic inspection of an austenitic stainless steel weld, Proceedings of the 6th ICNDE, M. Bieth and J. Whittle, Eds. EUR 23356 EN, European Commission, Budapest, October 2007, pp. 240-247.

[6] Chassignole B., Paris O. and Abittan E.: Ultrasonic examination of a CVCS weld, Proceedings of the 6th ICNDE, M. Bieth and J. Whittle, Eds. EUR 23356 EN, European Commission, Budapest, October 2007, pp. 764-772.

[7] Kemnitz P., Richter U., Klüber H.: Measurements of the acoustic field on austenitic welds, Nuclear Engineering and Design, 1997, vol. 174, no. 3, pp. 259-272.

[8] Engler O., Gottstein G.: A new approach in texture research: local orientation determination with EBSP, Steel Research, 1992, vol. 63, no. 9, pp. 413-418.

[9] Apfel A., Moysan J., Corneloup G., Fouquet T. and Chassignole B.: Coupling an ultrasonic propagation code with a model of the heterogeneity of multipass welds to simulate ultrasonic testing, Ultrasonics, 2005, vol. 43, no. 6, pp. 447-456.

[10] Becache E., Joly P. and Tsogka C.: An analysis of new mixed finite elements for the approximation of wave propagation problems, SIAM Journal of Numerical Analysis, 2000, vol. 37, no. 4, pp. 1053-1084.

[11] Chassignole B., Duwig V., Ploix M-A., Guy P. and El Guerjouma R.: Modelling the attenuation in the ATHENA finite elements code for the ultrasonic testing of austenitic welds, Ultrasonics, 2009, vol. 49, no. 8, pp. 653-658.

[12] Lhémery A., Calmon P., Lecoeur-Taïbi I., Raillon R. and Paradis L.: Modelling tools for ultrasonic inspection of welds, NDT&E International, 2000, vol. 33, no. 7, pp. 499-513.

[13] Mahaut S., Darmon A., Chatillon S., Jenson F. and Calmon P.: Recent advances and current trends of ultrasonic modelling in CIVA, Insight, 2009, vol. 51, no. 2, pp. 78-81.

[14] Ahmed S. and Thompson R.B.: Effect of preferred grain orientation and grain elongation on ultrasonic wave propagation in stainless steel, Review of Progress in Quantitative Non Destructive Evaluation, Proceedings of the 18th Annual Review, Brunswick, ME, July 28-Aug. 2, 1991 (A93-19582 06-38), vol. 11B, pp. 1999-2006.

[15] Chassignole B., Villard D., Dubuget M., Baboux J.C. and El Guerjouma R.: Characterization of austenitic stainless steel welds for ultrasonic NDT, Proceedings of Rewiew of Progress in QNDE, Montreal, July 1999, vol. 20B, pp. 1325-1332.

[16] Seldis T. and Pecorari C.: Scattering-induced attenuation of an ultrasonic beam in austenitic steel, The Journal of the Acoustical Society of America, 2000, vol. 108, no. 2, pp. 580-587.

[17] Diaz J., Schumm A., Duwig V., Fouquet T. and Chassignole B.: Structural noise in modelisation, Proceedings of 9th European Conference on NDT, Berlin, September 2006.

[18] Chassignole B., Dupond O., Doudet L., Duwig V. and Etchegaray N.: Ultrasonic examination of an austenitic weld: illustration of the disturbances of the ultrasonic beam, Proceedings of Review of Progress in QNDE, Chicago, July 2009, vol. 28B, pp. 1886-1893.

[19] Chassignole B., Dupond O. and Doudet L.: Ultrasonic and metallurgical examination on an alloy 182 welding mold, Proceedings of the 7th ICNDE, Yokohama, May 2009.

About the authors

Mr. Bertrand CHASSIGNOLE (bertrand.chassignole@edf.fr), Research engineer and Mr. Olivier DUPOND (olivier.dupond@edf.fr), Head of the Metallurgy Group, are both with the Materials and Mechanics of Components Department of EDF R&D, Moret-sur-Loing (France). Mr. Thierry FOUQUET (thierry.fouquet@edf.fr), Research engineer, is with the Department of Neutronics Simulation, Information Technologies and Scientific Calculations of EDF R&D, Clamart (France). Mr. Alain LE BRUN (alain.le-brun@edf.fr), Research engineer, is with the Department of Simulation and Treatment of Information of EDF R&D, Chatou (France). Mr. Joseph MOYSAN (joseph.moysan@univmed.fr), Professor, is with the Laboratory of Non Destructive Characterization of the Mediterranean University, Aix en Provence (France). Mr. Philippe BENOIST (philippe.benoist@cea.fr), Head of the LIST Department, is with the French Atomic Enegy Commission (CEA), Saclay (France).